Modelling the production of solid and liquid products from the hydrothermal carbonisation of two biomasses

A.M. Borrero-López, Éric Masson, Alain Celzard, Vanessa Fierro

Modelling the production of solid and liquid products from the hydrothermal carbonisation of two biomasses

A.M. Borrero-López[1], E. Masson[2], A. Celzard[1], V. Fierro[1*]

[1] Université de Lorraine, CNRS, IJL, F-88000 Épinal, France

[2] Critt bois, 27 rue Philippe Seguin, BP 91067, 88051 Épinal Cedex 9, France

[*] Corresponding author. Tel: + 33 372 74 96 77. Fax: + 33 372 74 96 38. E-mail address : Vanessa.Fierro@univ-lorraine.fr (V. Fierro)

Abstract

This work focuses on the hydrothermal carbonisation (HTC) of two bioresources, olive stones (OS) and beechwood (BW), within the ranges of temperature and time of 160-240ºC and 1-24 hours, respectively. The final pH of the liquid phase, the yields of solid and liquid, and the nature and amounts of a broad range of molecules (two furanic and nine phenolic compounds) were produced and studied. The experimental results obtained were discussed in relation to predictive equations developed in a previous study (Borrero-López et al., 2018) regarding the cellulose, hemicellulose and lignin contents of the two bioresources. Adequate fits were obtained for the pH of the liquid phase (9-11% overestimation for OS and BW, respectively), the yields of solid (7-8% error for OS and BW, respectively) and liquid (6-16% error for OS and BW, respectively) and the production of 5-hydroxymethylfurfural and several phenolic compounds, while some discrepancies for the production of furfural and a few phenolic compounds were observed but were properly analysed and discussed.

Keywords: olive stones; beechwood; modelling; hydrothermal carbonization; furfural, phenolics.

1. Introduction

Hydrothermal carbonisation (HTC) is attracting increasing interest because of the mild pressure and temperature conditions involved in this process (Liu et al., 2012), the production of valuable products in the aqueous phase (Guardia et al., 2019), and the possibility of using the hydrochars obtained as precursors of new carbonaceous (Yahia et al., 2019) or oxide materials (Kavil et al., 2019). Hydrothermal carbonisation of biomass is indeed a simple process in which bioresources are treated in hot pressurised water in an autoclave at moderate temperatures, within the typical range of 140-240ºC. Then, hydrothermal reactions occur at the medium pressures generated by water evaporation in the hermetically sealed autoclave (Borrero-López et al., 2018). The hydrochars produced when biomass was subjected to HTC have been used for soil conditioning (Bento et al., 2019), development of lubricants (Huang et al., 2019), stabilisation of Pickering emulsions (Xie et al., 2018), conversion to solid fuels (Lucian et al., 2018; Ma et al., 2018; Zhao et al., 2018), adsorbents (Lei et al., 2018), and metal detection (Liu et al., 2012).

In addition to hydrochar, the release of many valuable products from the main components of biomass, i.e., from hemicellulose, cellulose and lignin, is achieved through bond cleavage and self-catalysed reactions due to the presence of water (Borrero-López et al., 2017). Materials scientists often neglect the liquid phase although various phenolic compounds (Borrero-López et al., 2018), as well as furfural (FU) and 5-hydroxymethyl furfural (5-HMF) (Grote et al., 2018; Wataniyakul et al., 2018), can be obtained, making this phase a high-added value, cheap and safe source of chemicals (Borrero-López et al., 2018; Nakason et al., 2018; Zhao et al., 2018). However, products separation is still difficult and therefore, restricting production to a limited number of product by catalysis (Sun et al., 2018) seems a very interesting strategy. Moreover, the

63 importance and applications of FU and 5-HMF have been ubiquitously highlighted
64 (Borrero-López et al., 2017). Among the phenolic compounds, some interesting
65 chemicals such as vanillin and syringaldehyde have also been found (Rodrigues Pinto et
66 al., 2012, Borrero-López et al., 2017). Others, such as acetosyringone, guaiacylacetone,
67 guaiacol or syringol, have also been produced, all of them having noteworthy
68 antioxidant and antimicrobial activity (Conde et al., 2011; Gullón et al., 2017). Finally,
69 the production of gases at higher temperatures, usually catalysed by acids and/or metal,
70 has also been extensively studied (Salimi et al., 2018). In conclusion, HTC undoubtedly
71 is an outstanding biorefinery tool for converting lignocellulosic resources into valuable,
72 useful solid, liquid and gaseous products.

73 On the other hand, efforts have focused on understanding the kinetics of the involved
74 transformation mechanisms. Thus, Keiller et al. (2019) stated that hydrothermal
75 carbonisation may occur through direct reactions, often of first order, whereas others
76 have discussed the possibility of intermediates and side products (Borrero-López et al.,
77 2017; Gallifuoco et al., 2018; Gallifuoco and Di Giacomo, 2018; Zhao et al., 2018). The
78 modelling of HTC products was carried out by applied statistical methods (Gallifuoco
79 and Di Giacomo, 2018), response surface methodology (Heidari et al. (2019) and Zhao
80 et al., 2018) and process simulators (Gómez et al. (2019)). Overall, these studies require
81 powerful calculation tools in addition to the development of sophisticated models, due
82 to the complexity of kinetics (Marcotullio, 2011), as well as accurate experimental and
83 analytical studies. In a former work, the solid and liquid products obtained when
84 cellulose, hemicellulose and lignin were subjected to HTC have been meticulously
85 studied. Various models were presented that were able to predict solid and liquid yields,
86 the final pH of the liquid phase and the concentrations of FU, 5-HMF and several
87 phenolic products (Borrero-López et al., 2018).

The objective of the present study is to test the validity of these models when the entire lignocellulosic biomass, instead of its independent components, is submitted to HTC. To this end, olive stones (OS) (*Olea europaea*) and beechwood (BW) (*Fagus sylvatica*) have been subjected to HTC at temperatures ranging from 140 to 240ºC and durations ranging from 1 to 24 hours. The severity factor, which is a useful tool for understanding HTC, was used to simultaneously account for the effects of time and temperature. The experimental data were finally compared to the predictions of the models.

2. Materials and Methods

2.1. Raw materials

The cellulose, hemicellulose and lignin contents of OS and BW were determined according to the Tappi standards (T 264, T 203 and T 222, respectively). Each analysis was repeated three times and the average error was lower than 3%. More details can be found elsewhere (Borrero-López et al., 2017).

Olive stones (OS) were purchased at a local factory in Gabès (Tunisia) and ground at a size of less than 2 mm. The cellulose, hemicellulose and lignin contents were 40.5, 21.7 and 29.9 wt.%, respectively (Borrero-López et al., 2017). Beechwood (BW) was cut and milled and the resultant chips of an average size of less than 1 mm were recovered by using a powder collector. The corresponding cellulose, hemicellulose and lignin contents were 43.6, 33.5 and 22.1 wt.%, respectively.

All compounds used for identification and quantification of phenolic and furan compounds using HPLC equipment were analytical grade and purchased from Sigma-Aldrich (Steinheim, Germany).

2.2. Hydrothermal carbonisation

Hydrothermal carbonisation tests were performed according to the conditions established elsewhere (Borrero-López et al., 2018). In brief, 2 g of the selected biomass were introduced into a glass vial with 16 g of distilled water. The vial was then placed in a 100 mL Teflon-lined autoclave, sealed and placed in a preheated oven at the desired temperature (140-240ºC) for times ranging from 1 to 24h.

The combined effect of time and temperature on the process was taken into account through the severity factor, $logR_0$, (Overend and Chornet, 1987), as follows:

$$logR_0 = log\left[t \cdot exp\left(\frac{T-100}{\omega}\right)\right] \quad (1)$$

where the higher importance of temperature, T (°C), with respect to time, t (min), can be observed in the exponential dependence of R_0 on T and its linear dependence on t. Regarding the empirical parameter ω, a value of 14.75 has been traditionally used with lignocellulosic materials. However, it has been modified as needed to accommodate a variety of bioresources and temperatures (Kim et al., 2014; Ko et al., 2015). Table 1 shows the experimental conditions and consequent severity factors used for OS and BW.

Table 1. Performed tests and corresponding values of severity ($logR_0$).

Olive Stones		Beechwood	
Test conditions	$logR_0$	Test conditions	$logR_0$
160ºC, 6h	4.32	160ºC, 1h	3.54
170ºC, 2h	4.14	160ºC, 2h	3.85
170ºC, 4h	4.44	160ºC, 3h	4.02
170ºC, 6h	4.62	160ºC, 6h	4.32
180ºC, 2h	4.43	160ºC, 12h	4.62
180ºC, 4h	4.74	160ºC, 24h	4.92
180ºC, 6h	4.91	180ºC, 1h	4.13
190ºC, 4h	5.03	180ºC, 2h	4.43
190ºC, 6h	5.21	180ºC, 3h	4.61
190ºC, 8h	5.33	180ºC, 6h	4.91
200ºC, 2h	5.02	180ºC, 12h	5.21
200ºC, 4h	5.32	180ºC, 24h	5.51
200ºC, 6h	5.50	200ºC, 1h	4.72
220ºC, 2h	5.61	200ºC, 2h	5.02
240ºC, 1h	5.90	200ºC, 3h	5.20
240ºC, 2h	6.20	200ºC, 6h	5.50
		200ºC, 12h	5.80
		200ºC, 24h	6.10

2.3. Liquid/Solid separation

Upon completion of the HTC, the brownish solid, or hydrochar, was separated from the liquid by vacuum filtration and completely dried in a vacuum oven, where it was held for 6h at 60ºC before being weighed and stored. After separation, the liquid was also weighed and refrigerated to avoid further reactions until analysis.

2.4. Chromatographic analysis

The quantitative analysis of the main compounds in the liquid phase was carried out using an Ultimate 3000 high-performance liquid chromatograph (Thermo Fisher Scientific, Germany), coupled to an automatic sampler and with both diode array and fluorescence detectors. Two different columns were used for the appropriate separation and quantification of furan and phenolic compounds: Hypersyl Green PAH (Thermo

Fisher Scientific, Germany) and Pinnacle DB BiPh 5 μm (Restek, USA), respectively. The quantification of furans was performed at UV absorption wavelengths of 220, 276, 284 and 291 nm by selecting water and acetonitrile as mobile phases. For the determination of phenolic compounds, the same mobile phases were used, but 195, 201, 231 and 300 nm were the selected UV absorption wavelengths. More information on the analysis protocol can be found elsewhere (Borrero-López et al., 2018). The limits of detection for HPLC measurements were around 0.0004 g/L.

2.5. Yield analysis

The hydrochar and liquid-phase yields, i.e., Y_{HC} and Y_{LC}, respectively, were calculated according to the following equations (2) and (3):

$$Y_{HC}\ (\%) = \frac{W_{HC}}{W_{BC}} \times 100 \quad (2)$$

$$Y_{LC}\ (\%) = \frac{L}{L_0} \times 100 \quad (3)$$

where W_{HC} expresses the dry weight of the resultant hydrochar, W_{BC} is the initial weight of the biomass compound (BC) fed into the autoclave, L is the resultant liquid content after HTC, and L_0 is the initial amount of distilled water added.

2.6. Procedure to estimate HTC products

The present procedure is based on recent models (Borrero-López et al., 2018) initially developed to describe the behaviour of the three main biomass components: cellulose, hemicellulose and lignin, submitted to HTC separately, in terms of final pH, hydrochar and liquid yields, and concentrations in FU, 5-HMF and phenolic molecules. Based on these former models, we tried to assess whether it was possible to predict the final composition and yields of HTC products or the possible synergistic effects when the real biomass is submitted to HTC. For that purpose, we used two rather different

biomasses, OS and BW, the former being much richer in lignin than the latter. The final pH of the liquid phase reads as follows:

$$Final\ pH = p1 + p2\ (logR_0) + p3\ (logR_0)^2 \quad (4)$$

where *p1*, *p2* and *p3* are experimental parameters. A polynomial expression was then determined for each biopolymer: cellulose, hemicellulose and lignin.

The hydrochar yield from each biomass compound is as follows:

$$Y_{HC,BC} = \frac{Y_0 + Y_\infty\ (k\ logR_0)^m}{1 + (k\ logR_0)^m} \quad (5)$$

where the hydrochar yield of each lignocellulosic polymer ($Y_{HC,BC}$) depends on the constant initial and final hydrochar yields (Y_0 and Y_∞, respectively), and on two parameters, *k* and *m*, which account for the slope of the yield drop and the severity value at which the drop starts, respectively.

The concentrations of FU and 5-HMF produced when submitting biomass to HTC read, respectively:

$$Model\ A;\ C = C_{BC} \cdot \left(\frac{k_{1F}}{k_{3F} - k_{1F}}\right) \cdot \left[e^{-(k_{1F})\cdot t} - e^{-(k_{3F})\cdot t}\right] \quad (6)$$

$$Model\ B;\ C = C_{BC} \cdot \left(\frac{k_{1F}}{k_{3F} - k_{1F} - k_{2F}}\right) \cdot \left[e^{-(k_{1F}+k_{2F})\cdot t} - e^{-k_{3F}\cdot t}\right] \quad (7)$$

Both models were applied because the latter takes into account an intermediate in the production of FU from xylose. C_{BC} was the initial concentration of the BC (cellulose, hemicellulose or lignin) while k_1, k_2 and k_3 were the constants corresponding to the various reactions taking place.

The concentrations of the following phenolic molecules produced from lignin read as follows:

Vanillin, syringaldehyde and acetosyringone:

$$C_{phenolic\ compound} = a + b(logR_0) + c(logR_0)^2 \quad (8)$$

188 Guaiacyalcetone:

189 $$C_{phenolic\ compound} = \alpha + \beta(logR_0) \quad (9)$$

190 Syringol, guaiacol and phenol production:

191 $$C_{phenolic\ compound} = \delta + B \cdot e^{(\kappa(logR_0))} \quad (10)$$

192 where a determined set of parameters has been developed for each compound.

193 Using the corresponding model and taking into account the lignocellulosic
194 composition of both OS and BW, the aforementioned yields and concentrations of the
195 main HTC products were estimated.

196 **2.7. Relative error analysis**

197 To determine to what extent the various models match the real data, the following
198 expression was used to calculate the relative error:

199 $$error\ \% = \frac{|V_{th} - V_{exp}|}{V_{exp}} \cdot 100 \quad (11)$$

200 where V_{exp} and V_{th} are respectively the experimental and predicted data, whether for pH
201 value, hydrochar or liquid yields, or concentration of a given product obtained during
202 the HTC of OS or BW.

203

3. Results

3.1. Final pH of the liquid phase

The final pH after HTC gives information on the severity of the process and on the reactions that have taken place. Fig. 1a shows the pH of the liquid fraction after HTC of OS and BW along with the predicted data obtained.

Figure 1

As can be seen, the pH of the liquid fraction after HTC was generally higher for BW than for OS within the studied range of severity, which is in good agreement with their lignocellulosic composition. At low severity, the higher the cellulose and hemicellulose contents, the higher the pH final values (Borrero-López et al., 2018). In the former paper it was shown that, as severity increases, lignin produces a slight increase in the final pH, cellulose decreases it considerably, and hemicellulose gives a minimum of about pH 5. Therefore, the experimental results observed represent a clear combination of the degradations of the three biopolymers. Although a slight overestimation of pH was observed (about +9% and +11% for OS and BW, respectively), the predicted evolution of pH with severity followed the same trend as the experimental one.

3.2. Hydrochar yield

Fig. 1b shows the values of $Y_{HC,BC}$ for OS and BW. At low severity, $Y_{HC,BW}$ was higher than $Y_{HC,OS}$ due to the higher cellulose content of BW, a biopolymer that was found to lead to the highest yields under these conditions (Borrero-López et al., 2018). Nevertheless, at the highest severities, lignin began to play a more significant role in the hydrochar yield, leading to values of $Y_{HC,OS}$ closer to those of $Y_{HC,BW}$.

The differences between the predicted and experimental $Y_{HC,BC}$ were as low as about 7% and 8% for OS and BW, which shows the relevance of the proposed equation for predicting the yield of hydrochar of two very different biomasses submitted to HTC.

3.3. Liquid yield

Fig. 2a shows the liquid yield for both biomasses, that of OS being higher than that of BW due to its higher lignin and lower cellulose contents, respectively. Nevertheless, due to the high hemicellulose content of BW, the two datasets were very similar. In our former work (Borrero-López et al., 2018), no model could be obtained for the liquid yields from the HTC of hemicellulose, cellulose and lignin, due to the scattering of the results. However, the experimental liquid yields of lignin, cellulose and hemicellulose and the corresponding compositions were used here to predict the results. Thus, for each severity value and for each bioresource, the liquid yields previously obtained from raw cellulose, hemicellulose and lignin were weighed with the lignocellulose concentration, generating the predicted values. In spite of that impossibility to previously obtain a proper model (Borrero-López et al., 2018), the predicted data were found to be in very good agreement with the OS liquid yield, with an average error of about 6%; however, the BW liquid yield was slightly overestimated, with an average error of 16%.

Fig. 2b shows the differences between experimental and predicted values from the model. The general overestimation of the liquid yield, especially for BW, can be explained by some synergistic effect that may occur when the three biopolymers are linked together. As a result, some reactions can be hindered and the extraction of water from the raw biomass can be limited. In addition, it can be concluded that both cellulose and hemicellulose must be responsible for this higher resistance to HTC, because OS,

with a higher lignin content, does not present such an overestimation of liquid yield (Xiao et al., 2012).

Figure 2

3.4. Concentrations of FU and 5-HMF and estimates

Fig. 3 shows the concentrations of FU and 5-HMF experimentally produced from OS and BW. Unexpectedly, the FU concentration from OS was significantly higher than that from BW. Such a finding was surprising because BW contains a much higher fraction of hemicellulose, which is directly responsible for the production of FU. Moreover, the latter from both materials was much higher than expected, based on their hemicellulose content and our previous study (Borrero-López et al., 2018), as clearly seen in Fig. 3a and 3b, which also show the predictions of models A and B. This can be explained because higher concentrations of pentoses are known to be responsible for side reactions, so the lower hemicellulose concentration of both biomasses may actually increase the yields (Marcotullio, 2011). In addition, since FU is generally produced under acid-catalysed conditions (Dashtban et al., 2012; Matsagar et al., 2017), cellulose degradation, which produces a substantial decrease in pH, can potentially enhance the production of FU from OS and BW compared to hemicellulose itself. Moreover, the lower pH reported for OS can also explain the difference between the two biomasses. The FU yields obtained are in the range of other studies, as already shown in a previous work (Borrero-López et al., 2017).

Figure 3

Regarding 5-HMF production, overall, the predictions were closer to the experimental data than for FU. Nonetheless, it is worth mentioning the extremely high overestimation shown by model A when considering a constant calculated from the

equations (data not shown). The production of 5-HMF was higher for BW for almost all the considered severity factors, which was consistent with its higher cellulose content when compared to OS. Nevertheless, the highest 5-HMF production was obtained from OS at the highest tested severity factor. In summary, the most reliable predictions obtained were those considering equations developed from the application of model B.

3.5. Concentrations of phenolic compounds and estimates

It is well known that lignin can produce a wide range of phenolic compounds from the decomposition of its structure into its constituent units (Borrero-López et al., 2018; Cesari et al., 2019; Yang et al., 2019). In the present work, nine different types of phenolic compounds have been identified and quantified for OS and BW, the concentrations of which have also been estimated by application of the previous models developed from HTC tests on lignin (Borrero-López et al., 2018). These phenolic compounds are vanillin, guaiacylacetone, syringol, syringaldehyde, guaiacol, acetosyringone, phenol, acetovanillone and creosol. Only the first seven compounds were plotted in Fig. 4 for OS and BW, because the concentrations of acetovanillone and creosol were below the limits of detection (0.0005 and 0.0004 mg/L, respectively) throughout the whole range of conditions studied. The absence of creosol was somehow expected, since previous studies on the HTC of lignin only produced it at severities greater than 6 (Borrero-López et al., 2018). However, the concentration of acetovanillone had comparable values to syringaldehyde (Borrero-López et al., 2018), thus the production of acetovanillone should be somewhat limited by the synergistic action of both cellulose and hemicellulose and the corresponding reduction of pH.

Figure 4

Since the concentration of lignin in OS is the highest, one would think that the concentrations of phenolic compounds from this bioresource would be the highest. However, similar to what occurred with FU production, this was true only for vanillin, guaiacylacetone and final phenol concentration, while the remaining phenolic compounds concentrations from OS were similar to or less than from BW. This fact highlights the extreme importance of the lignin content, which may vary significantly from one bioresource to another. Since the concentration of monolignols and other units may be very different, different concentrations of the resulting products can be obtained (Anderson et al., 2019; Santos et al., 2015a; Santos et al., 2015b). Both OS and BW derive from hardwoods, thus close syringyl(S) / guaiacyl(G) (p-hydroxyphenylpropane) ratios are expected. Some authors (Simon et al., 2014) have reported that BW has a S/G ratio close to 1, while others suggest lower ratios that depend on the extraction process (Choi et al., 2001). In contrast, the OS S/G ratio was postulated at 1.08 (Harman-Ware et al., 2015). On the contrary, the lignin used for modelling was PROTOBIND 1075, which comes from softwood, so that the S/G ratio drops dramatically to very low values depending on the initial biomass (Anderson et al., 2019), which makes the structure of lignin completely different. Therefore, this fact may compromise the accuracy of the model (Borrero-López et al., 2018; Li et al., 2013; Sameni, 2015).

Nevertheless, the predicted data showed adequate fits for the vast majority of them, highlighting the validity and adaptability of the model. However, here again, the influence of the simultaneous HTC of the remaining lignocellulosic biopolymers affects the prediction of the results by modifying the interactions and modifying the composition of the liquid phase. Thus, in our previous work, it has been shown how the final pH from lignin HTC increased with severity (Borrero-López et al., 2018), although, for the bioresources studied in this work, the final pH has decreased as a result

of the presence of both cellulose and hemicellulose. Thus, the compounds that depend on acidic or basic catalysis can have a completely different behaviour, as shown for vanillin, acetosyringone, acetovanillone and syringaldehyde, whose concentration was generally overestimated as a result of low pH.

In addition, the general underestimation observed for syringyl-derived units may also result from the higher S/G ratio of hardwoods, with respect to softwoods, which is known to facilitate the effectiveness of delignification (Anderson et al., 2019; Schmetz et al., 2019).

4. Conclusions

The hydrothermal carbonisation of OS and BW was successfully performed in a wide range of severity factor values. pH, hydrochar and liquid yields as well as some furan and phenolic compounds were determined, and the experimental results were compared to estimates. These estimates were obtained taking into account the hemicellulose, cellulose and lignin contents of the biomasses as well as the results of the fits obtained for the same parameters when these components of biomass were separately submitted to HTC. The following general trends could be derived.

- The final pH of liquids derived from BW was generally higher than that measured in OS-derived liquids, which is in good agreement with their lignocellulosic composition. An average overestimate of 10% of the pH value was obtained because of the synergistic effect between the three lignocellulosic compounds, but the trends were well predicted.
- A similar trend was observed in the hydrochar yield although the agreement between predicted and experimental values was much better (around 7%).

- The liquid yield was higher for the OS because of its higher lignin and lower cellulose contents. A good fit was obtained, reaching about 6 and 16% average error for OS and BW, respectively.
- Extremely high concentrations were obtained for FU, which is attributable to lower rates of side reactions and the influence of the final pH. The concentrations of 5-HMF were lower, and a better approximation was obtained with model B. The concentrations of phenolic compounds were of the same order as those predicted, but highly dependent on the selected biomass and pH.

Although further analysis is needed to explain the unexpected concentrations of FU, the models predicted trends similar to those determined experimentally. A systematic study in which mixtures of biomass components would be submitted to HTC would be necessary to understand the undergoing reaction mechanisms and synergistic effects.

Declaration of interest

The authors declare no competing financial interest.

Acknowledgements

This work was supported by a grant overseen by the French National Research Agency (ANR) as part of the "Investissements d'Avenir" program (ANR-11-LABX-0002-01, Lab of Excellence ARBRE) and TALiSMAN project, funded by FEDER (2019-000214). A.M.B-L. acknowledges the Ph.D. Research Grant received from the Ministerio de Educación, Cultura y Deporte (FPU16/03697).

Bibliography

Anderson, E.M., Stone, M.L., Katahira, R., Reed, M., Muchero, W., Ramirez, K.J., Beckham, G.T., Román-Leshkov, Y., 2019. Differences in S/G ratio in natural poplar variants do not predict catalytic depolymerization monomer yields. Nat. Commun. 10, 2033. https://doi.org/10.1038/s41467-019-09986-1

Bento, L.R., Castro, A.J.R., Moreira, A.B., Ferreira, O.P., Bisinoti, M.C., Melo, C.A., 2019. Release of nutrients and organic carbon in different soil types from hydrochar obtained using sugarcane bagasse and vinasse. Geoderma 334, 24–32. https://doi.org/10.1016/j.geoderma.2018.07.034

Borrero-López, A M, Fierro, V., Jeder, A., Ouederni, A., Masson, E., Celzard, A., 2017. High added-value products from the hydrothermal carbonisation of olive stones. Environ. Sci. Pollut. Res. 24, 9859–9869. https://doi.org/10.1007/s11356-016-7807-6

Borrero-López, A.M., Masson, E., Celzard, A., Fierro, V., 2018. Modelling the reactions of cellulose, hemicellulose and lignin submitted to hydrothermal treatment. Ind. Crops Prod. 124, 919–930. https://doi.org/10.1016/j.indcrop.2018.08.045

Cesari, L., Mutelet, F., Canabady-rochelle, L., 2019. Antioxidant properties of phenolic surrogates of lignin depolymerisation. Ind. Crop. Prod. 129, 480–487. https://doi.org/10.1016/j.indcrop.2018.12.010

Choi, J.W., Faix, O., Meier, D., 2001. Characterization of Residual lignins from chemical pulps of spruce (*Picea abies L.*) and beech (*Fagus sylvatica L.*) by

analytical pyrolysis-gas chromatography/mass spectrometry. Holzforschung 55, 185–192. https://doi.org/10.1515/HF.2001.031

Conde, E., Moure, A., Domínguez, H., Parajó, J.C., 2011. Production of antioxidants by non-isothermal autohydrolysis of lignocellulosic wastes. LWT - Food Sci. Technol. 44, 436–442. https://doi.org/10.1016/j.lwt.2010.08.006

Dashtban, M., Gilbert, A., Fatehi, P., 2012. Production of furfural: overview and challenges. J-For. 2, 44-53.

Gallifuoco, A., Di Giacomo, G., 2018. Novel kinetic studies on biomass hydrothermal carbonization. Bioresour. Technol. 266, 189–193. https://doi.org/10.1016/j.biortech.2018.06.087

Gallifuoco, A., Taglieri, L., Scimia, F., Papa, A.A., Di Giacomo, G., 2018. Hydrothermal conversions of waste biomass: Assessment of kinetic models using liquid-phase electrical conductivity measurements. Waste Manag. 77, 586–592. https://doi.org/10.1016/j.wasman.2018.05.033

Gómez, J., Corsi, G., Pino-Cortés, E., Díaz-Robles, L.A., Campos, V., Cubillos, F., Pelz, S.K., Paczkowski, S., Carrasco, S., Silva, J., Lapuerta, M., Pazo, A., Monedero, E., 2019. Modeling and simulation of a continuous biomass hydrothermal carbonization process. Chem. Eng. Commun. https://doi.org/10.1080/00986445.2019.1621858

Grote, F., Ermilova, I., Lyubartsev, A.P., 2018. Molecular Dynamics Simulations of Furfural and 5-Hydroxymethylfurfural at Ambient and Hydrothermal Conditions. J. Phys. Chem. B 122, 8416–8428. https://doi.org/10.1021/acs.jpcb.8b03350

Guardia, L., Suárez, L., Querejeta, N., Rodríguez Madrera, R., Suárez, B., Centeno, T.A., 2019. Apple Waste: A Sustainable Source of Carbon Materials and Valuable Compounds. ACS Sustain. Chem. Eng. 7, 17335–17343. https://doi.org/10.1021/acssuschemeng.9b04266

Gullón, B., Eibes, G., Moreira, M.T., Dávila, I., Labidi, J., Gullón, P., 2017. Antioxidant and antimicrobial activities of extracts obtained from the refining of autohydrolysis liquors of vine shoots. Ind. Crops Prod. 107, 105–113. https://doi.org/10.1016/j.indcrop.2017.05.034

Harman-Ware, A.E., Crocker, M., Pace, R.B., Placido, A., Morton III, S., DeBolt, S., 2015. Characterization of Endocarp Biomass and Extracted Lignin Using Pyrolysis and Spectroscopic Methods. Bioenergy Res. 8, 350–368. https://doi.org/10.1007/s12155-014-9526-5

Heidari, M., Norouzi, O., Salaudeen, S., Acharya, B., Dutta, A., 2019. Prediction of Hydrothermal Carbonization with Respect to the Biomass Components and Severity Factor. Energy and Fuels 33, 9916–9924. https://doi.org/10.1021/acs.energyfuels.9b02291

Huang, J., Li, Y., Jia, X., Song, H., 2019. Preparation and tribological properties of core-shell Fe3O4@C microspheres. Tribol. Int. 129, 427–435. https://doi.org/10.1016/j.triboint.2018.08.036

Kavil, J., Anjana, P.M., Roshni, C.P., Periyat, P., Raj, K.G., Rakhi, R.B., 2019. Multifunctional nanohybrid material from discarded razor blades as cost-effective supercapacitor electrodes and oil-spill cleaners. Appl. Surf. Sci. 487, 109–115. https://doi.org/10.1016/j.apsusc.2019.05.055

Keiller, B.G., Muhlack, R., Burton, R.A., Van Eyk, P.J., 2019. Biochemical Compositional Analysis and Kinetic Modeling of Hydrothermal Carbonization of Australian Saltbush. Energy and Fuels 33, 12469–12479. https://doi.org/10.1021/acs.energyfuels.9b02931

Kim, Y., Kreke, T., Mosier, N.S., Ladisch, M.R., 2014. Severity Factor Coefficients for Subcritical Liquid Hot Water Pretreatment of Hardwood Chips. Biothecnol. Bioeng. 111, 254–263. https://doi.org/10.1002/bit.25009

Ko, J.K., Kim, Y., Ximenes, E., Ladisch, M.R., 2015. Effect of liquid hot water pretreatment severity on properties of hardwood lignin and enzymatic hydrolysis of cellulose. Biotechnol. Bioeng. 112, 252–262. https://doi.org/10.1002/bit.25349

Lei, Y., Su, H., Tian, F., 2018. A Novel Nitrogen Enriched Hydrochar Adsorbents Derived from Salix Biomass for Cr (VI) Adsorption. Sci. Rep. 8, 4040. https://doi.org/10.1038/s41598-018-21238-8

Li, Y., Cui, D., Tong, Y., Xu, L., 2013. Study on structure and thermal stability properties of lignin during thermostabilization and carbonization. Int. J. Biol. Macromol. 62, 663–669. https://doi.org/10.1016/j.ijbiomac.2013.09.040

Liu, S., Tian, J., Wang, L., Zhang, Y., Qin, X., Luo, Y., Asiri, A.M., Al-Youbi, A.O., Sun, X., 2012. Hydrothermal treatment of grass: A low-cost, green route to nitrogen-doped, carbon-rich, photoluminescent polymer nanodots as an effective fluorescent sensing platform for label-free detection of Cu(II) ions. Adv. Mater. 24, 2037–2041. https://doi.org/10.1002/adma.201200164

Lucian, M., Volpe, M., Gao, L., Piro, G., Goldfarb, J.L., Fiori, L., 2018. Impact of hydrothermal carbonization conditions on the formation of hydrochars and

455 secondary chars from the organic fraction of municipal solid waste. Fuel 233, 257–
456 268. https://doi.org/10.1016/j.fuel.2018.06.060

457 Ma, Q., Han, L., Huang, G., 2018. Effect of water-washing of wheat straw and
458 hydrothermal temperature on its hydrochar evolution and combustion properties.
459 Bioresour. Technol. 269, 96–103. https://doi.org/10.1016/j.biortech.2018.08.082

460 Marcotullio, G., 2011. The Chemistry and Technology of Furfural Production in
461 Modern Lignocellulose-Feedstock Biorefineries.
462 http://resolver.tudelft.nl/uuid:a307ecb3-513a-4f57-b519-873a73403cfd (accessed
463 18 December 2019)

464 Matsagar, B.M., Hossain, S.A., Islam, T., Alamri, H.R., Alothman, Z.A., Yamauchi, Y.,
465 Dhepe, P.L., Wu, K.C.W., 2017. Direct Production of Furfural in One-pot Fashion
466 from Raw Biomass Using Brønsted Acidic Ionic Liquids. Sci. Rep. 7, 13508.
467 https://doi.org/10.1038/s41598-017-13946-4

468 Nakason, K., Panyapinyopol, B., Kanokkantapong, V., Viriya-empikul, N., Kraithong,
469 W., Pavasant, P., 2018. Hydrothermal carbonization of unwanted biomass
470 materials: Effect of process temperature and retention time on hydrochar and liquid
471 fraction. J. Energy Inst. 91, 786–796. https://doi.org/10.1016/j.joei.2017.05.002

472 Overend, R.P., Chornet, E., 1987. Fractionation of Lignocellulosics by Steam-Aqueous
473 Pretreatments. Philos. Trans. R. Soc. A 321, 523–536.
474 https://doi.org/10.1098/rsta.1987.0029

475 Rodrigues Pinto, P.C., Borges da Silva, E.A., Rodrigues, A.E., 2012. Lignin as Source
476 of Fine Chemicals: Vanillin and Syringaldehyde. In: Baskar C., Baskar S., Dhillon
477 R. (eds) Biomass Conversion. Springer, Berlin, Heidelberg, pp. 381-420.

Salimi, M., Tavasoli, A., Balou, S., Hashemi, H., Kohansal, K., 2018. Influence of promoted bimetallic Ni-based catalysts and Micro/Mesopores carbonaceous supports for biomass hydrothermal conversion to H2-rich gas. Appl. Catal. B Environ. 239, 383–397. https://doi.org/10.1016/j.apcatb.2018.08.039

Sameni, J.K., 2015. Physico-Chemical Characterization of Lignin Isolated from Industrial Sources for Advanced Applications. http://hdl.handle.net/1807/70871 (accessed 18 December 2019)

Santos, J.I., Martín-Sampedro, R., Fillat, Ú., Oliva, J.M., Negro, M.J., Ballesteros, M., Eugenio, M.E., Ibarra, D., 2015a. Evaluating lignin-rich residues from biochemical ethanol production of wheat straw and olive tree pruning by FTIR and 2d-nmr. Int. J. Polym. Sci. 2015, 314891. https://doi.org/10.1155/2015/314891

Santos, J.I., Fillat, Ú., Martín-Sampedro, R., Ballesteros, I., Manzanares, P., Ballesteros, M., Eugenio, M.E., Ibarra, D., 2015b. Lignin-enriched Fermentation Residues from Bioethanol Production of Fast-growing Poplar and Forage Sorghum. BioResources 10, 5215–5232. https://doi.org/10.15376/biores.10.3.5215-5232

Schmetz, Q., Teramura, H., Morita, K., Oshima, T., Richel, A., Ogino, C., Kondo, A., 2019. Versatility of a Dilute Acid/Butanol Pretreatment Investigated on Various Lignocellulosic Biomasses to Produce Lignin, Monosaccharides and Cellulose in Distinct Phases. ACS Sustain. Chem. Eng. 7, 11069–11079. https://doi.org/10.1021/acssuschemeng.8b05841

Simon, M., Brostaux, Y., Vanderghem, C., Jourez, B., Paquot, M., Richel, A., 2014. Optimization of a formic/acetic acid delignification treatment on beech wood and its influence on the structural characteristics of the extracted lignins. J. Chem. Technol. Biotechnol. 89, 128–136. https://doi.org/10.1002/jctb.4123

Sun, Z., Fridrich, B., De Santi, A., Elangovan, S., Barta, K., 2018. Bright Side of Lignin Depolymerization: Toward New Platform Chemicals. Chem. Rev. 118, 614–678. https://doi.org/10.1021/acs.chemrev.7b00588

Wataniyakul, P., Boonnoun, P., Quitain, A.T., Kida, T., Laosiripojana, N., Shotipruk, A., 2018. Preparation of hydrothermal carbon acid catalyst from defatted rice bran. Ind. Crops Prod. 117, 286–294. https://doi.org/10.1016/j.indcrop.2018.03.002

Xiao, L.P., Shi, Z.J., Xu, F., Sun, R.C., 2012. Hydrothermal carbonization of lignocellulosic biomass. Bioresour. Technol. 118, 619–623. https://doi.org/10.1016/j.biortech.2012.05.060

Xie, X., Wang, Y., Li, X., Wei, X., Yang, S., 2018. Pickering emulsions stabilized by amphiphilic carbonaceous materials derived from wheat straw. Colloids Surfaces A Physicochem. Eng. Asp. 558, 65–72. https://doi.org/10.1016/j.colsurfa.2018.08.063

Yahia, S.H., Keat Lee, K., Ayed, B., Church, T.L., Hedin, N., 2019. Activated Carbons from Hydrothermal Carbons Prepared in Milk. Sci. Rep. 9, 16956. https://doi.org/10.1038/s41598-019-53361-5

Yang, S., Fan, D., Li, G., 2019. Analysis of phenolic compounds obtained from bamboo microwave liquefaction for fast-curing phenol-formaldehyde resin preparation. J. Appl. Polym. Sci. 136, 46952. https://doi.org/10.1002/app.46952

Zhao, K., Li, Y., Zhou, Y., Guo, W., Jiang, H., Xu, Q., 2018. Characterization of hydrothermal carbonization products (hydrochars and spent liquor) and their biomethane production performance. Bioresour. Technol. 267, 9–16. https://doi.org/10.1016/j.biortech.2018.07.006

Figure Captions

Fig. 1. a) Final pH of the liquid phase; and b) hydrochar yield after HTC of OS and BW. The dashed lines represent the predicted values from the models.

Fig. 2. a) Experimental liquid yields for OS and BW; b) Differences between experimental and predicted values from the models.

Fig. 3. Concentrations of FU and 5-HMF produced from OS (a & c) and BW (b & d). The dashed lines represent the predicted values from the models.

Fig. 4. Phenolic compounds concentration from OS (left) and BW (right). The dashed red lines are predicted data from modelling and lignin content of the bioresource.

Figure 1

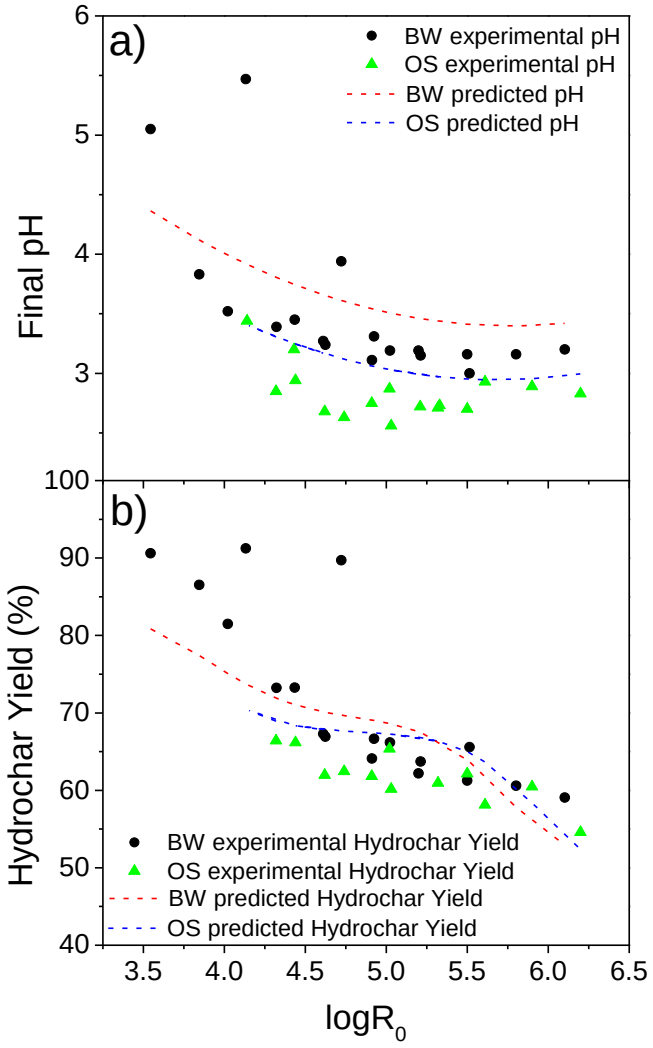

a) Final pH of the liquid phase; and b) hydrochar yield after HTC of OS and BW. The dashed lines represent the predicted values from the models.

Figure 2

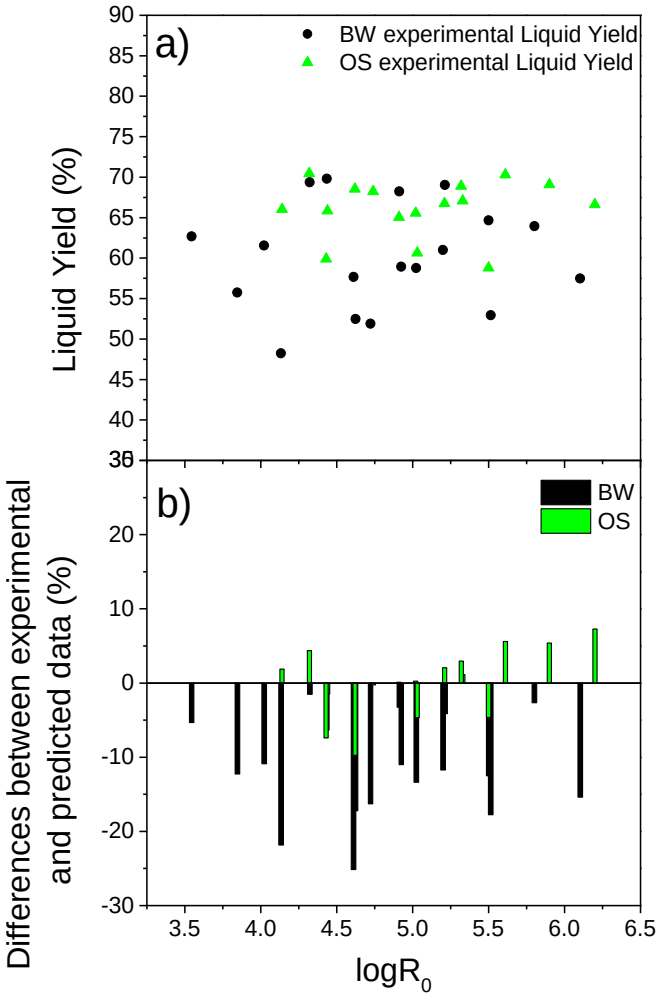

a) Experimental liquid yields for OS and BW; b) Differences between experimental and predicted values from the models.

550

551 Figure 3

552

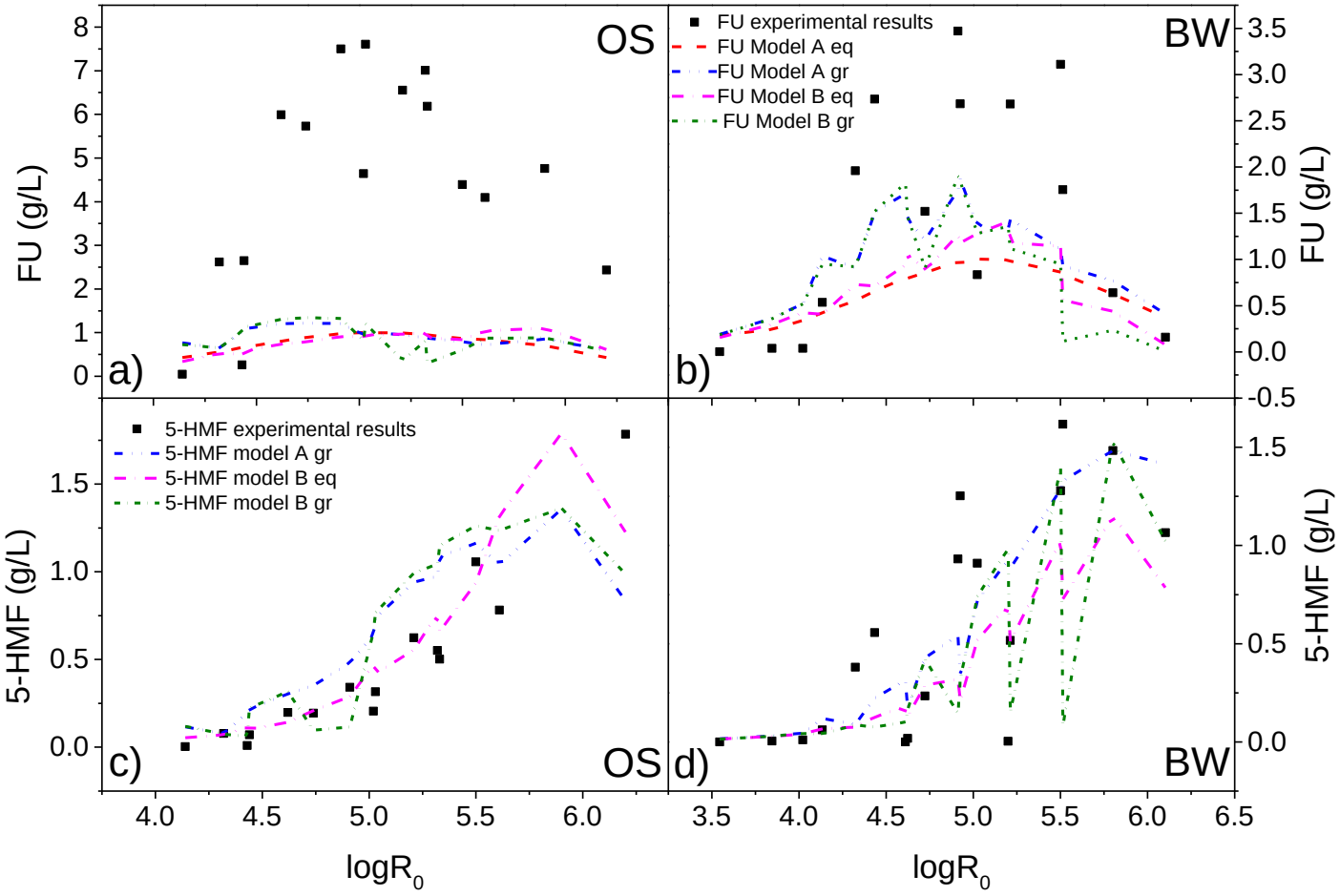

553
554

555 Concentrations of FU and 5-HMF produced from OS (a & c) and BW (b & d). The

556 dashed lines represent the predicted values from the models.

557

Figure 4

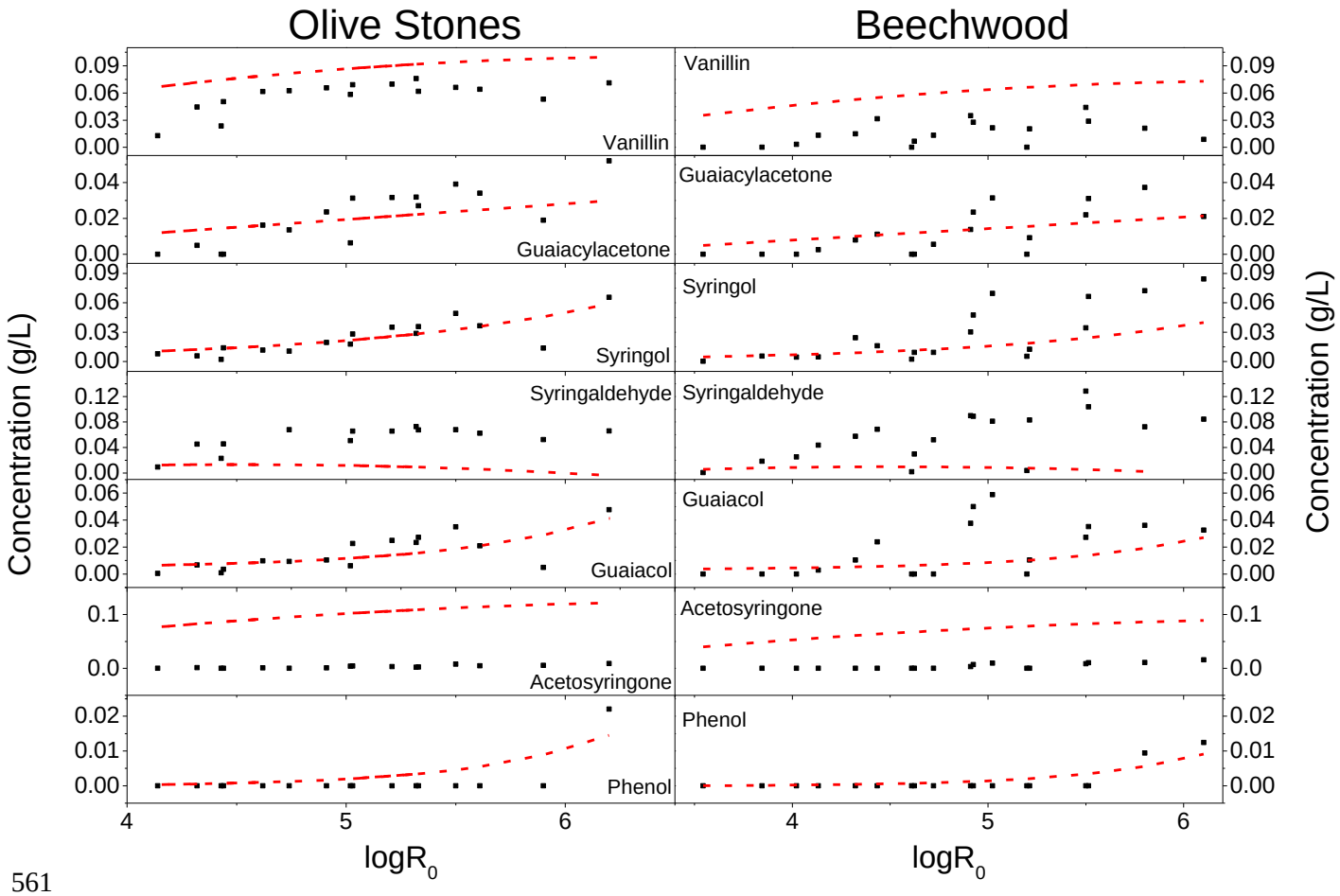

Phenolic compounds concentration from OS (left) and BW (right). The dashed red lines are predicted data from modelling and lignin content of the bioresource.